Materials **2014**, *7*, 6028-6044; doi:10.3390/ma7086028

OPEN ACCESS

materials

ISSN 1996-1944

www.mdpi.com/journal/materials

Article

A Novel Magnetic Graphene Oxide Composite Absorbent for Removing Trace Residues of Polybrominated Diphenyl Ethers in Water

Ning Gan *, Jiabing Zhang, Shaichai Lin, Nengbing Long, Tianhua Li and Yuting Cao *

The State Key Laboratory Base of Novel Functional Materials and Preparation Science, Faculty of Material Science and Chemical Engineering of Ningbo University, Ningbo 315211, Zhejiang, China; E-Mails: hcchcnc@126.com (J.Z.); xg1012@126.com (S.L.); longnengbing@nbu.edu.cn (N.L.); litianhua@nbu.edu.cn (T.L.)

* Authors to whom correspondence should be addressed;
E-Mails: ganning@nbu.edu.cn (N.G.); caoyuting@ nbu.edu.cn (Y.C.);
Tel.: +86-574-8760-9983 (N.G.); Fax: +86-574-8760-0734 (N.G.);
Tel./Fax: +86-574-6164-2147 (Y.C.).

Received: 8 May 2014; in revised form: 29 May 2014 / Accepted: 8 August 2014 / Published: 21 August 2014

Abstract: The purpose of the study was to develop a facile method for the fabrication of a stable and reusable magnetic graphene composite absorbent to remove trace levels of polybrominated diphenyl ethers in water treatment. The poly cationic Fe_3O_4@PDDA (poly(diallyldimethyl ammonium chloride) (PDDA)) core-shell structured nanoparticles were first synthesized, and then, DNA was laid on the surface of graphene oxide (GO*x*) to prepare the polyanionic GO*x*@DNA composite. The above materials were then mixed together and adhered together through sol-gel technology. Thus, the Fe_3O_4@PDDA/GO*x*@DNA composite absorbent was prepared. Its performance was tested by disperse solid phase extraction and gas chromatography/mass spectrometric (GC/MS) for removing six kinds of indicative polybrominated diphenyl ethers (BDEs) in water samples. The removal percentages of several real samples for six kinds of BDEs (BDE17, BDE28, BDE 71, BDE 47, BDE 66, BDE 100) at the ng/mL order of magnitude were in the range of 88.2%–99.1%. The removal percentage still reached 80.0% when the adsorbent was reused at least 20 times. The results suggested that the magnetic absorbent can obviously remove trace levels of BDEs from large volumes of aqueous solutions in environmental pollution cleanup with high removal efficiency.

Keywords: graphene oxide; magnetic disperse solid phase extraction; water treatment; sol-gel technology; polybrominated diphenyl ethers

1. Introduction

Polybrominated biphenyls (BDEs) have been widely applied in many areas, including heat transfer fluids and dielectric fluids [1]. However, they are a typical class of the persistent organic pollutants (POPs) that cause great harm to the environment, as well as human health, due to their toxicity, high stability and biomagnification through the food chain [1]. Because of their low aqueous solubility and bioavailability, BDEs are resistant to biodegradation and are difficult to be removed by conventional physicochemical techniques, such as coagulation, flocculation, sedimentation and filtration [2]. Therefore, it is necessary to remove organic dyes in environmental water. Adsorption has been regarded as one of the most effective physical processes for removing BDEs in wastewaters, since it can produce high quality water and also be a process that is economically feasible. Activated carbon (AC) is the most widely used commercially available absorbent [3]. However, difficult regeneration and lower absorption capacity limits its application in waste water treatment [4].

Carbon nanotubes and graphene oxide (GO*x*) are a class of electron-rich carbon adsorbents with a large delocalized π-electron system, which shows promising applications in water treatment [5]. Due to grapheme oxide's unique plate structure and properties, including large specific surface area, excellent stability and rich functionalities [6], organic compounds with a benzene ring can be strongly adsorbed on GO*x*. However, a major defect comes from the difficulties that are associated with the separation of water-insoluble GO*x* from water solutions after absorption procedures. Magnetic composite materials also have many advantages, such as simple separation, high adsorption capacity and cyclic utilization, which can greatly expand their application in environmental purification. Magnetic separation has been developed to facilitate the collection of GO*x* [7,8].

Various magnetic materials can be used as adsorbents. Fe_3O_4@PDDA (poly(diallyldimethyl ammonium chloride) (PDDA)) with a core-shell structure can form magnetic nanoparticles that reveal excellent dispersion and chemical stability, which are not easy to reunite and for saturation magnetization. The sol-gel technique will be selected as the preparation method for combining Fe_3O_4@PDDA with positive charges and GO*x*@DNA, which has a large amount of negative charges [7,8]. In the preparation process, oppositely-charged species are deposited on a carrier in sequences through electrostatic assembly [8]. In this study, the Fe_3O_4@PDDA core-shell-structured nanoparticles were modified with GO*x*@DNA through sol-gel technology in order to improve their stability and adsorption capacity. Herein, the magnetic microspheres with Fe_3O_4 as the core and PDDA on its surface as a shell were synthesized through the sol-gel approach, which can obtain polycationic magnetic microspheres (Fe_3O_4@PDDA). The above materials were modified with polyanionic graphenes, which were modified by negative DNA. In the composites, the polyelectrolyte layer cannot only enhance the adhesive strength between GO*x*@DNA and Fe_3O_4@PDDA, but also increase the amount of the GO*x* on it.

Combined with magnetic nanocomposites (Fe_3O_4@PDDA/GO*x*@DNA) as adsorbents, the technique of magnetic solid-phase extraction (mSPE) was chosen for an effective pretreatment assay to enrich and purify analytes in samples with a complex matrix [9–15]. With the magnetic property, the new absorbent using mSPE could avoid time-consuming procedures and be performed directly to pretreat crude samples without the need for centrifugation or filtration, due to the facile magnetic separation [10]. The aim of this study was to develop a simple, rapid, inexpensive and robust methodology to remove BDEs in real water samples. The proposed methodology included magnetic nanocomposites (Fe_3O_4@PDDA/GO*x*@DNA) prepared by sol-gel technology for removing BDEs in environmental water samples. The adsorption experiment showed that the magnetic nanocomposites could be reused at least 20 times without a significant loss of the clean-up efficiency. The adsorbents were successfully employed for removing the trace level of BDEs in real water samples.

2. Materials and Methods

2.1. Chemicals

2,4-Dibromophenyl 2-bromophenyl ether (BDE17), 2,4,4′-tribromodiphenyl ether (BDE28), 2,3′,4′,6-tetrabromodiphenyl ether (BDE 71), 2,2′,4,4′-tetrabromodiphenyl ether (BDE 47), 2,3′,4,4′-tetrabromodiphenyl ether (BDE 66) and 2,2′,4,4′,6-pentabromodiphenyl ether (BDE 100) were obtained from Accu Standard Inc. (New Haven, CT, USA). Ct-DNA (Lot: D4522-1MG, Sigma, New York, NY, USA) and poly(diallyldimethyl ammonium chloride) (PDDA, 20%, w/w, in water, MW = 100,000–200,000) were purchased from Sigma-Aldrich (New York, NY, USA). The carboxyl of graphenes (purity > 95 wt%, ASH < 1.5 wt%, SSA > 500 m^2/g) were purchased from Nanoport. Co. Ltd. (Shenzhen, China). Ferric chloride ($FeCl_3 \cdot 6H_2O$), ammonia (28%), *n*-hexane, ethylene glycol, tetraethyl orthosilicate (TEOS), sodium acetate and dichloromethane were purchased from Beijing Chemicals Corporation (Beijing, China). The syringe filters were purchased from Xingya (Shanghai, China). All other chemicals were used as received without further purification. The water in this work was deionized water.

2.2. Preparation of Fe_3O_4@PDDA/GOx@DNA Nanoparticles

2.2.1. Synthesis of Fe_3O_4 Nanospheres

The magnetic nanoparticles were prepared based on the previously reported hydrothermal procedures [11]. 5.75 g $FeCl_3 \cdot 6H_2O$ and 15.33 g of sodium acetate were dissolved in 320 mL of ethylene glycol under mechanical stirring. The obtained homogeneous yellow solution was transferred to a Teflon-lined stainless steel autoclave, sealed and heated at 200 °C for 8 h. The obtained black magnetite precipitate was washed with ethanol and deionized water three times, then dried at 60 °C under vacuum.

2.2.2. Synthesis of Fe_3O_4@PDDA Nanospheres

The Fe_3O_4@PDDA nanospheres were prepared according to the previously reported sol-gel method [12]. Briefly, 0.5 g of dry Fe_3O_4 particles were firstly pretreated with 0.1 M HCl aqueous

solution (100 mL) by ultrasonication for 15 min. Moreover, pH 7.0 PBS was added to maintain the neutral characteristics. The resulting suspension was stirred in 0.1 mol/L PDDA for 6 h at room temperature. The obtained Fe_3O_4@PDDA nanospheres were magnetically separated, washed with ethanol and deionized water, then dried at 60 °C in vacuum for 2 h. The black precipitate was washed with deionized water three times and dried at 60 °C in vacuum for 2 h.

2.2.3. Synthesis of Fe_3O_4@PDDA/GO*x*@DNA Nanoparticles

Graphene was firstly purified in 0.5 M HCl solution by ultrasonication for 4 h. The resulting material was washed with water several times and dried under vacuum at 60 °C overnight [13]. 50 mg purified GO*x* were dispersed in sodium chloride aqueous solution (0.5 mol/L, 100 mL). Then, 6 mL of DNA solution (20%) were added dropwise under vigorous stirring. The mixture was centrifuged at 5000 rpm for 5 min and washed with deionized water to remove the superfluous DNA. The obtained GO*x*/DNA with a positive charge was dried at 60 °C in vacuum overnight.

Fifty milligrams of Fe_3O_4@PDDA nanoparticles with a negative charge were dispersed in 100 mL of water. Then, 50 mg of dry GO*x*/DNA were added with mechanical stirring. After reaction for 60 min, the product was collected with a magnet, then washed with ethanol and deionized water, dried at 60 °C in vacuum for 2 h. The preparation process is shown in Figure 1.

Figure 1. Synthesis strategy of Fe_3O_4@PDDA /GO*x*@DNA.

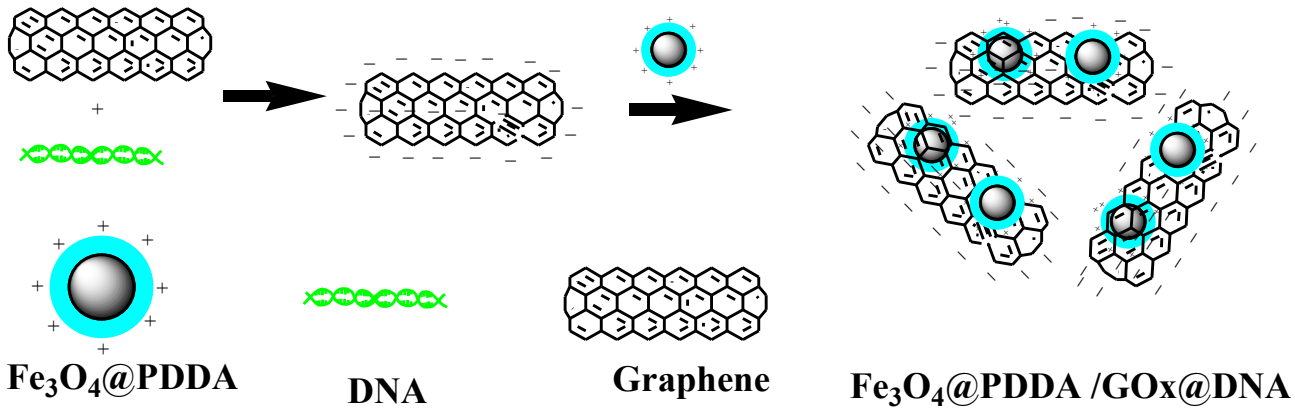

2.3. The Removal Experiment for BDEs in Waters

Sample solutions (1000 ng/mL) with six kinds of BDEs were prepared in isooctane and stored at 4 °C. All of the working solutions of BDEs were 100 ng/mL and prepared daily by appropriate dilution of the stock solutions with *n*-hexane. All glassware used in the study was soaked and washed in acetone, then rinsed with *n*-hexane and dried at 100 °C for 4 h.

For the adsorption steps, 30 mg of the adsorbents (Fe_3O_4@PDDA/GO*x*@DNA) were rinsed and activated in 1 mL of methanol, then uniformly dispersed into the 100-mL filtered water sample in a beaker (100 mL of deionized water spiked with 10 ng/mL of BDEs were used, and all of the experiments were performed in triplicate). The mixture was stirred vigorously at 300 rpm for 30 min. Subsequently, a strong magnet was placed at the bottom of the beaker, so that the adsorbents were isolated from the solution. The solution became limpid after about 1 min. The procedures are shown in Figure 2.

Figure 2. The absorption and detection process to remove the polybrominated biphenyls (BDEs) in water.

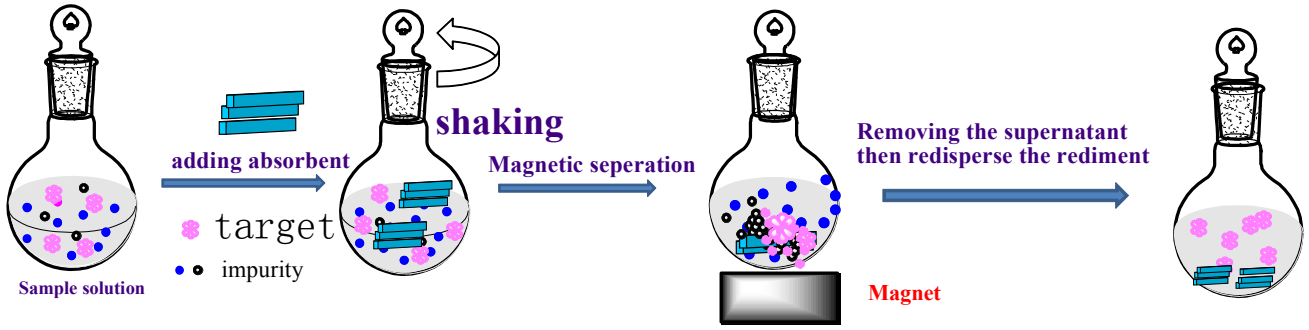

For the desorption step, firstly, the supernatant was decanted carefully with the magnet, and the pre-concentrated analytes were transferred to the syringes of an organic membrane (0.45 μm) and dried at 60 °C under vacuum for 4 h. Secondly, the adsorbed compounds were eluted from the adsorbents with 10 mL of a mixture of *n*-hexane:dichloromethane (40/60, v/v) as the elute. The flow rate was controlled at 2 mL/min, and the eluates were collected with a centrifugal tub. Thirdly, the adsorbents were dried with nitrogen to remove the dichloromethane and *n*-hexane. Then, the residue was dissolved in 1 mL of *n*-hexane with 0.5 mL of concentrated sulfuric acid to further acidification. Finally, the mixed solution was centrifuged for 10 min, and the supernatant liquid was stored in a fridge overnight. One microliter of this solution was injected into the GC/MS system for analysis. The experiment process is shown in Figure 2. The overall procedure took place at room temperature. The BDE removal percentage was calculated using Equation (1) [16].

$$\text{Removal percentage (\%)} = \frac{C_0 - C_t}{C_0} \times 100\% \quad (1)$$

where C_0 is the original concentration of BDEs and C_t *r*epresents the residual concentration of BDEs after extraction, respectively.

2.4. Real Sample Preparation

Water samples were collected in Ningbo in September, 2013. Tap water samples were taken from our laboratory in Yongjiang River, and water samples were acquired from Jiangbei District (Ningbo). All samples were collected randomly and filtered through 0.45-μm membranes to remove suspended particles.

3. Results and Discussion

3.1. Characterization of Adsorbents

SEM figures were used to characterize the morphology of Fe_3O_4, Fe_3O_4@PDDA, GO*x*@DNA and Fe_3O_4@PDDA/GO*x*@DNA (Figure 3a–d). Figure 3a shows that the mean particle size of Fe_3O_4 NPs was about 300 nm. Figure 3b shows the Fe_3O_4@PDDA cross-linked together, which proved that PDDA as a polymer was successfully coated onto Fe_3O_4 NPs. The tree-like structure of SEM images

(Figure 3c) of GO*x*@DNA showed that GO*x*@DNA was successfully synthesized. Both the feathery and spherical composite structures in Figure 3d also proved that GO*x*@DNA was successfully absorbed on the surface of Fe_3O_4@PDDA through sol-gel technology.

Figure 3. SEM images of: (**a**) Fe_3O_4; (**b**) Fe_3O_4@PDDA; (**c**) GO*x*@DNA; (**d**) Fe_3O_4@PDDA/GO*x*@DNA.

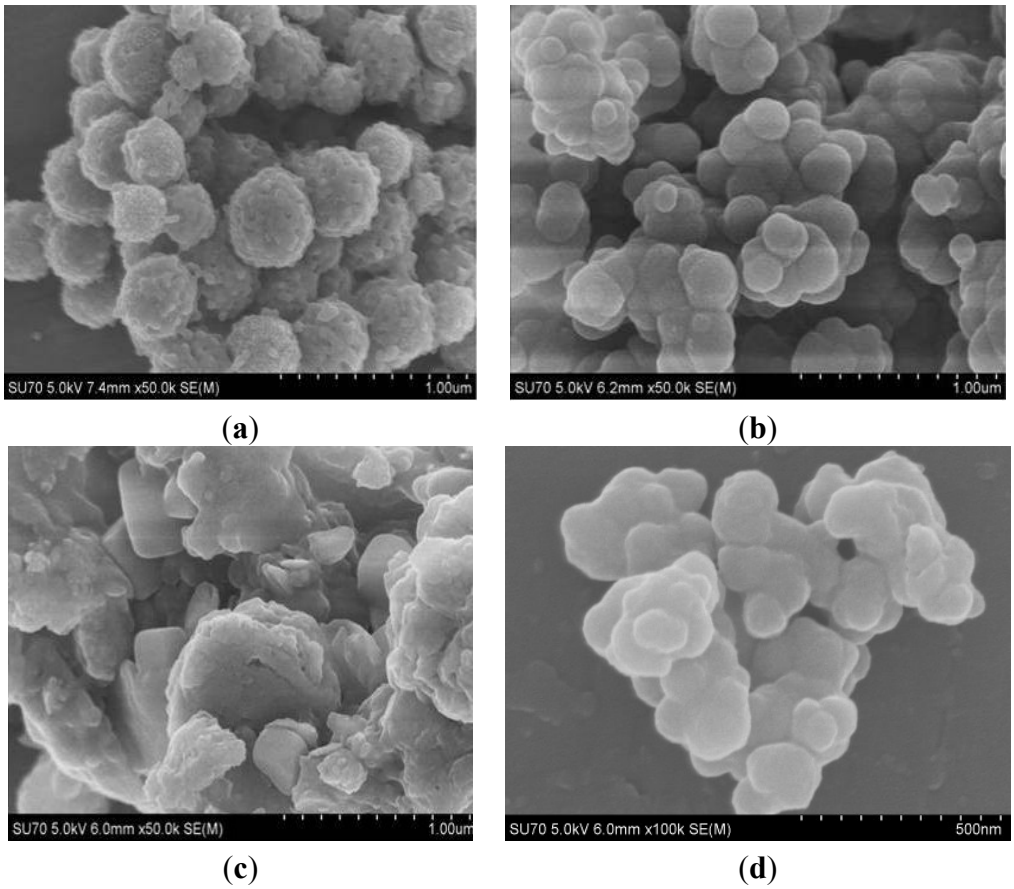

(**a**) (**b**)

(**c**) (**d**)

Figure 4 displayed the IR spectra of GO*x*, Fe_3O_4, Fe_3O_4@PDDA and Fe_3O_4@PDDA/GO*x*@DNA. Strong absorption bands between 3300 and 3500 cm^{-1} were due to O–H stretching vibration. The types of peaks shown by GO*x* were between 1300 and 1100 cm^{-1}, which were due to the stretching of phenyl-carbonyl C–C bonds. The 2924 and 2820 cm^{-1} bands were due to C–H (Figure 4a). As shown in Figure 4b, the peaks at 584 and 467 cm^{-1} were the stretching vibration due to the Fe–O bonds. Compared to the two spectra (Figure 4b,c), the Fe–O peaks shift to 580 and 473 cm^{-1} (Figure 4c). From Figure 4c,d, we could see that the C–H stretching vibrating band of Fe_3O_4@PDDA/GO*x*@DNA at 2924 and 2820 cm^{-1} appeared. All of these demonstrated that GO*x* was successfully modified to the Fe_3O_4@PDDA through sol-gel technology.

Figure 5 shows the magnetization curves of Fe_3O_4, Fe_3O_4@PDDA and Fe_3O_4@PDDA/GO*x*@DNA at room temperature. Maximum saturation magnetization of Fe_3O_4@PDDA was measured at 25.4 emu/g, which was lower than that of magnetic Fe_3O_4 alone (48.2 emu/g). This might be due to the nonmagnetic surface of the PDDA. The saturation magnetization of Fe_3O_4@PDDA/GO*x*@DNA was at 18.2 emu/g. Although the addition of the nonmagnetic part (GO*x*) led to a decrease in the saturation magnetizations, the obtained Fe_3O_4@PDDA/GO*x*@DNA still had a high saturation magnetization.

It was observed that Fe_3O_4@PDDA/GO*x*@DNA adsorbents could be dispersed into water solution readily. Thus, the magnetic adsorbents loaded with analytes could be isolated from the matrix conveniently by using an external magnet when necessary.

Figure 4. IR spectra of: (**a**) GO*x*; (**b**) Fe_3O_4; (**c**) Fe_3O_4@PDDA; (**d**) Fe_3O_4@PDDA/GO*x*@DNA.

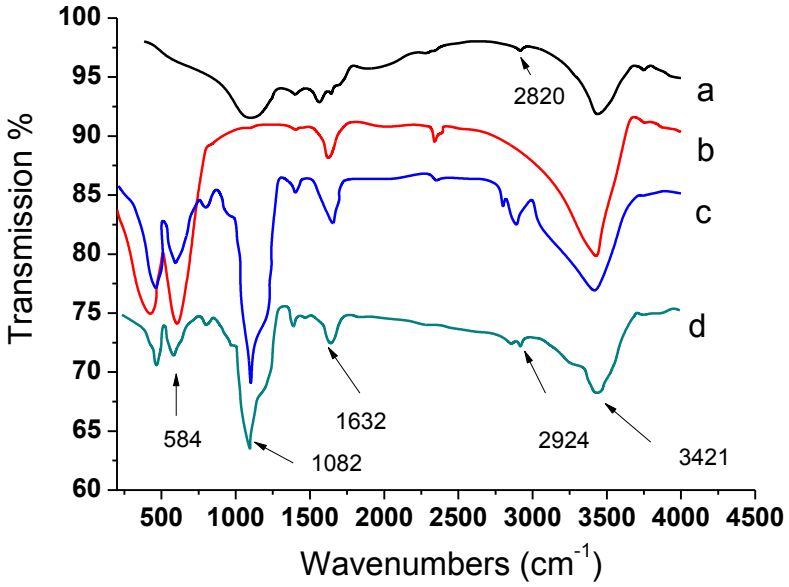

Figure 5. Vibrating sample magnetometer (VSM) magnetization curves of: (**a**) Fe_3O_4; (**b**) Fe_3O_4@PDDA; (**c**) Fe_3O_4@PDDA/GO*x*@DNA.

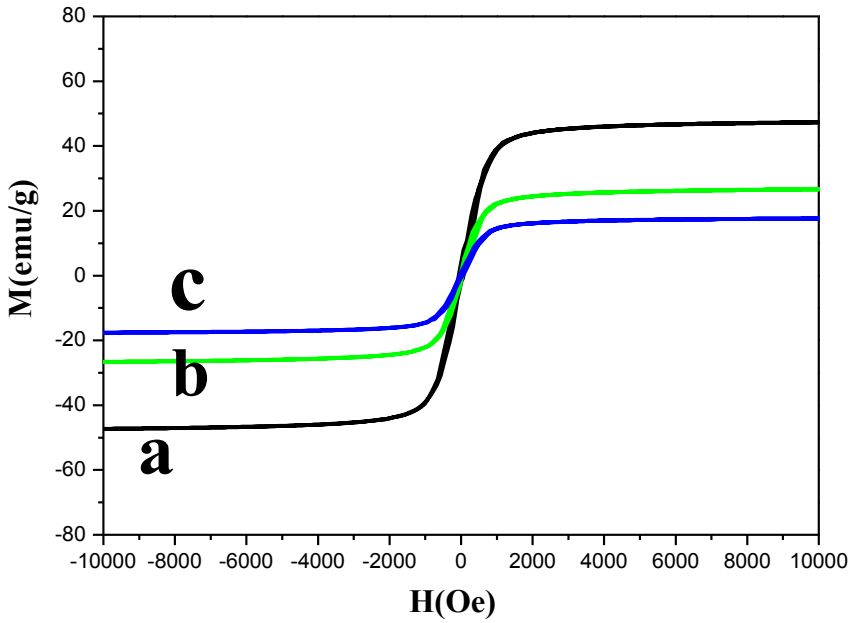

The XRD pattern in Figure 6a–d showed the crystal structure of the materials, GO*x*, Fe_3O_4, Fe_3O_4@PDDA and Fe_3O_4@PDDA/GO*x*@DNA, respectively. The well-resolved diffraction peak revealed the crystallinity of the GO*x*, which was located at 2θ = 22.5°. There were several relatively strong diffraction peaks at 2θ = 30.2°, 35.5°, 43.3°, 57.3° and 62.7° in Figure 6b, which were quite

similar to those of the Fe_3O_4 nanoparticles reported by other groups [14]. From the XRD pattern of Fe_3O_4@PDDA/GO*x*@DNA in Figure 6e, the main characteristic peaks of Fe_3O_4 still remained and the strong diffraction peak at 2θ = 22.5° (GO*x*) appeared again, which indicated that the composite was composed of Fe_3O_4@PDDA and GO*x*@DNA.

Figure 6. X-ray diffraction (XRD) patterns of: (**a**) GO*x*; (**b**) Fe_3O_4; (**c**) Fe_3O_4@PDDA; (**d**) Fe_3O_4@PDDA/GO*x*@DNA.

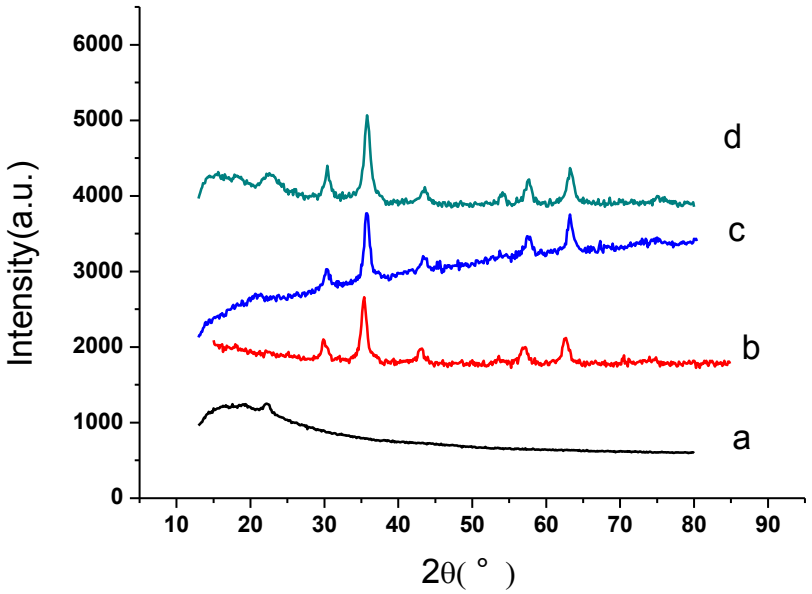

3.2. Kinetic Study

As shown in Figure 7a, the kinetics of the uptake of BDE28 by the Fe_3O_4@PDDA/GO*x*@DNA (100 mL of deionized water spiked with 152 ng/mL onto 30 mg of the adsorbents) was studied from the adsorption rate of BDE28 to the adsorbents, which showed two stages, a quick stage at the beginning and a slow stage before the equilibrium. The results (Figure 7a) showed that the rate of adsorption for BDE28 was very rapid in the first 20 min; thereafter, it decreased gradually, until it reached a plateau after 30 min, indicating the equilibrium of the system. The phenomena of the adsorption kinetics may be due to the adsorption of BDE28 on the exterior surface of the adsorbent at the initial period of contact time. When the adsorption on the exterior surface reached the saturation point, BDE28 reached into the pores of the adsorbent. In order to elucidate the adsorption process, the results were fitted using the Lagergren first-order model [17] and the pseudo second-order model [18]. The Lagergren first-order model can be expressed as follows:

$$\ln (Q_{eq} - Q_t) = \ln Q_1 - k_1 t \quad (2)$$

where k (min^{-1}) is the rate constant of adsorption and Q_t (mg g^{-1}) and Q_{eq} (mg g^{-1}) represent the amount of the dye adsorbed at any time t (min) and at equilibrium, respectively. The rate constant k can be determined from the slope of the plot obtained by plotting ln ($Q_{eq} - Q_t$) *versus* t.

The pseudo-second-order model equation is given as:

$$\frac{t}{Q_t} = \frac{1}{k_2 Q_{eq}^2} + \frac{t}{Q_{eq}} \quad (3)$$

where k_1 (min^{-1}) and k_2 (g mg^{-1} min^{-1}) are the rate constant of the Lagergren first-order model and pseudo-second-order model, Q_t (mg g^{-1}) and Q_{eq} (mg g^{-1}) represent the amount of the dye adsorbed at any time t (min) and at equilibrium and Q_1 (mg g^{-1}) and Q_2 (mg g^{-1}) are the calculated adsorption capacity of the Lagergren first-order model and pseudo-second-order model.

The Lagergren first-order rate constant k_1 and Q_1 can be determined from the intercept and slope of the plot obtained by plotting ln ($Q_{eq} - Q_t$) *versus* t; the pseudo-second-order rate constant k_2 and Q_2 can be determined from the intercept and slope of the plot obtained by plotting t/Q_t *versus* t.

The calculated parameters for Lagergren first-order model and pseudo-second-order model and the correlation coefficients (r^2) are listed in Table 1.

Table 1. Kinetic parameters for adsorption of BDE28 onto Fe_3O_4@PDDA/GO*x*@DNA.

Sample	Q_{eq} (mg g^{-1})	Lagergren First-Order Model			Pseud Second-Order Model		
		Q_1 (mg g^{-1})	K_1 (min^{-1})	r^2	Q_2 (mg g^{-1})	k_2 (g mg^{-1} min^{-1})	r^2
BDE28	49.1	49.0	0.387	0.998	49.1	0.023	0.984

Figure 7. The effect of adsorption time on the adsorption capacity.

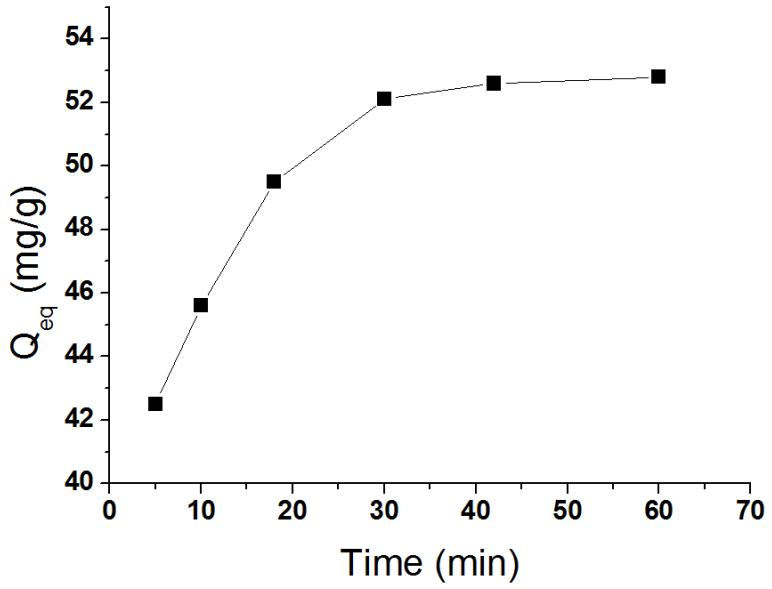

A comparison of Q_{eq} data (Table 2) shows that the calculated Q_2 values of the pseudo-second-order equation are generally closer to the experimental Q_{eq} values compared to the calculated Q_1 values of the Lagergren first-order equation. The correlation coefficients for the first order kinetic model obtained for all of the studied BDE28 were above 0.998. Therefore, the adsorption process studied follows the Lagergren first-order model better. Based on the assumption of the pseudo-second-order model [18], it can be concluded from the experimental result that the adsorption of cationic BDE28 on G-SO_3H/Fe_3O_4 is mainly due to chemical adsorption [19].

Table 2. Removal percentages of six kinds of BDEs from real water samples spiked with target analytes.

	Analytes	BDE17	BDE28	BDE71	BDE47	BDE66	BDE100
Tap water	Found (ng/mL)	ND	ND	ND	ND	ND	ND
	Removal percentages (%) (Add 5 ng/mL)	92.5 ± 2.3	94.1 ± 3.1	87.8 ± 2.9	93.2 ± 2.8	93.3 ± 3.9	90.2 ± 3.4
	Removal percentages (%) (Add 5 ng/mL)	92.3 ± 1.8	97.1 ± 1.3	95.2 ± 3.2	95.3 ± 3.1	88.9 ± 4.2	89.7 ± 3.2
Zhenhai River Water 1	Found (ng/mL)	1.62	1.53	1.42	ND	ND	ND
	Removal percentages (%) (Add 5 ng/mL)	90.2 ± 3.4	93.2 ± 4.8	92.1 ± 4.3	93.4 ± 3.2	89.5 ± 3.5	90.4 ± 3.3
	Removal percentages (%) (Add 5 ng/mL)	89.6 ± 1.8	89.7 ± 3.4	90.6 ± 3.4	90.7 ± 2.1	98.8 ± 3.4	93.5 ± 3.2
Yongjiang River water	Found (ng/mL)	1.42	1.21	ND	ND	ND	ND
	Removal percentages (%) (Add 5 ng/mL)	92.8 ± 2.1	97.5 ± 1.2	93.3 ± 3.2	92.4 ± 4.3	94.1 ± 3.1	93.3 ± 1.7
	Removal percentages (%) (Add 5 ng/mL)	92.3 ± 2.8	99.5 ± 2.9	94.1 ± 5.8	92.5 ± 4.7	92.3 ± 4.9	89.1 ± 2.8

ND: not detected.

3.3. Adsorption Isotherms

The adsorption isotherm gave the most significant information, which pointed out how the adsorbate molecules were distributed between the liquid phase and solid phase when the adsorption process reaches equilibrium. The adsorption isotherm helped to disclose the adsorption mechanism of BDE28 onto Fe_3O_4@PDDA/GO*x*@DNA. According to previous reports, the stronger adsorption of aromatic compounds on GOx was attributed to the π–π interaction. In addition, the hydrophobic effect was another important factor that was responsible for the adsorption on GO*x*. The adsorption of BDE28 on Fe_3O_4@PDDA/GO*x*@DNA was studied under ambient conditions using a batch technique. In the removal of BDE28 from aqueous solutions, the amount of adsorbents used in the cleaning procedure was vital for the economic application. In our study, the experimental data of BDE28 were fitted by employing the Langmuir and Freundlich model [20–22].

The form of the Langmuir isotherm can be represented by the following equation:

$$\frac{1}{q_e} = \frac{1}{q_{\max}} + \frac{1}{bq_{\max}} \cdot \frac{1}{c_e} \tag{4}$$

Here, $q_{\max}$ and b were Langmuir constants related to the adsorption capacity and adsorption energy, respectively. The standard correlation coefficient (R^2) was employed to compare the goodness of fit between model prediction and experimental data. The calculated values of $q_{\max}$ and $1/b$ were 49.1 mg/g and 4.2, respectively; R^2 was 0.998. The Freundlich isotherm model is expressed as follows:

$$\log q_e = \log k_F + n \log c_e \tag{5}$$

where k_F represents the adsorption capacity when the adsorbate equilibrium concentration equals one and n represents the degree of adsorption dependence at the equilibrium concentration.

The experimental data was not in good agreement with the Freundlich isotherm model after calculation (Figure 8). The absorbent had a high nitrogen BET specific area of ~310 m^2/g (calculated in the linear relative pressure range from 0.1 to 0.3) [22]. The average pore size was 3 nm, which showed it was microporous.

Figure 8. Freundlich isotherm for the adsorption of BDE28 to Fe_3O_4@PDDA/GO*x*@DNA.

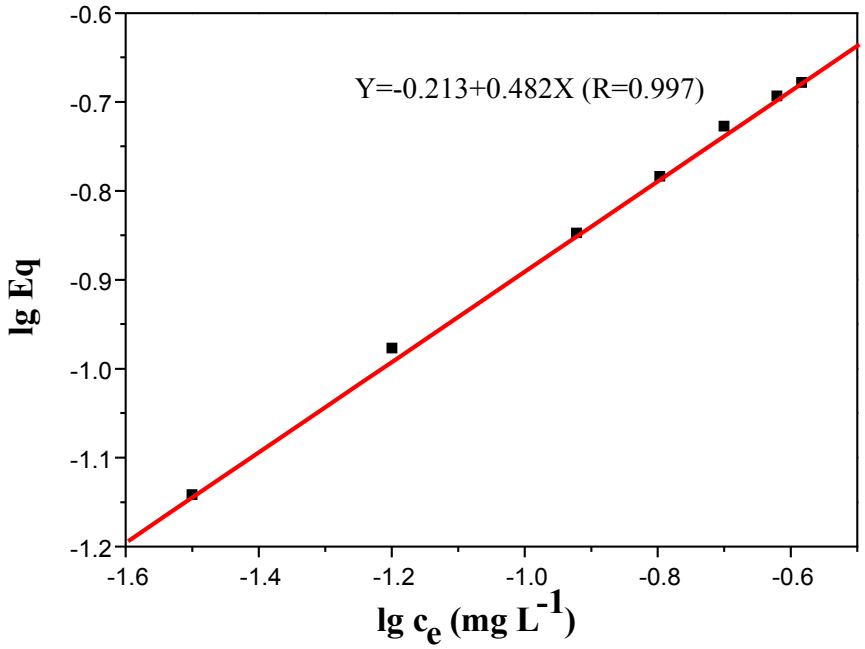

3.4. Effect of Adsorption Conditions

In this experiment, several parameters, including adsorption conditions and desorption conditions, were discussed to achieve the best removal efficiency for BDEs. To study the extraction performance of the mSPE under different experimental conditions, 100 mL of deionized water spiked with 10 ng/mL of BDEs were used, and all of the experiments were performed in triplicate. The results were used as a means of optimization.

3.4.1. Adsorption Time

In order to assess the ability of the Fe_3O_4@PDDA/GO*x*@DNA to adsorb BDE28, equilibrium adsorption time profiles were derived by increasing the adsorption time of 100 mL of the water sample. The results showed that there was a rapid removal efficiency when the adsorption time increased from 5 to 50 min. After 30 min, the maximum removal percentages were obtained for BDE28, which were close to 90% (Figure 9). Consequently, an adsorption time of 30 min was selected for further study.

Figure 9. The effect of the adsorption time on the adsorbed amount of BDE28 by Fe_3O_4@PDDA/GO*x*@DNA.

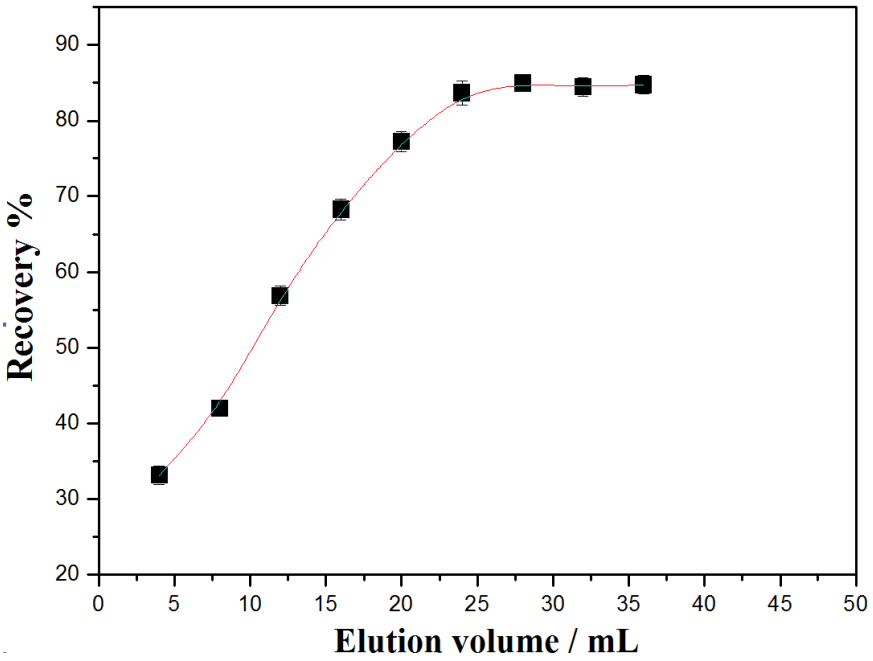

3.4.2. Amount of the Adsorbents

To achieve the highest maximum removal percentages towards the target analytes, the amount of Fe_3O_4@PDDA/GO*x*@DNA was increased from 5 mg to 50 mg. The overall recoveries were augmented significantly when the amount of adsorbents increased up to 20 mg; when the amount of adsorbents achieved 30 mg (Figure 10), the removal percentages of BDEs were exceeded by 85%.

Figure 10. The effect of the mount of the adsorbents on the recovery of BDE28 by Fe_3O_4@PDDA/GO*x*@DNA.

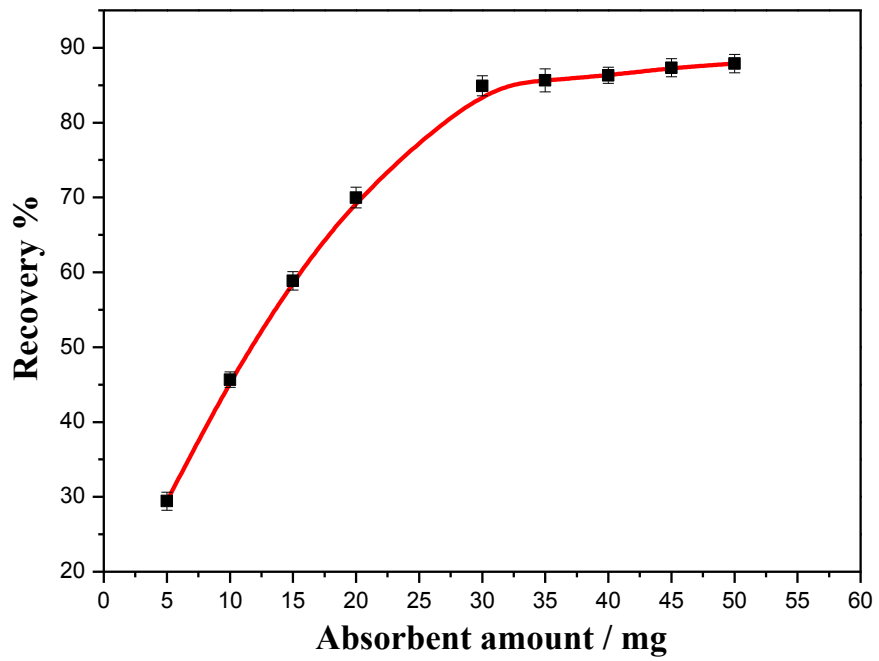

The overall removal percentages were made to remain unchanged by further increasing the amount of the adsorbents, indicating the remarkable enrichment ability of Fe_3O_4@PDDA/GO*x*@DNA as adsorbents. Thirty milligrams of the adsorbents were employed in the study by considering the sensitivity and consumption of the material.

3.4.3. Effect of the Solution pH

The pH was adjusted between 3.0 and 11.0 by the addition of 0.1 M HCl or NaOH. The adsorption percentage of BDEs on Fe_3O_4@PDDA/GO*x*@DNA fluctuated very little with the recovery ranging from 80% to 85% in a pH range of 5–10, with a lower recovery between pH 2 to 3 (Figure 11). All of this suggested that the analytes could efficiently be adsorbed onto the adsorbent at any pH of the real neutral aqueous solutions. Since the pH of the real water samples was generally in the range 5.0–8.0, there was no need to adjust the pH of the sample solution before adsorption. As seen from our experiment, the absorbent was suitable for PCB pollution cleanup in real work.

Figure 11. The effect of pH on the recovery of BDE28 by Fe_3O_4@PDDA/GO*x*@DNA.

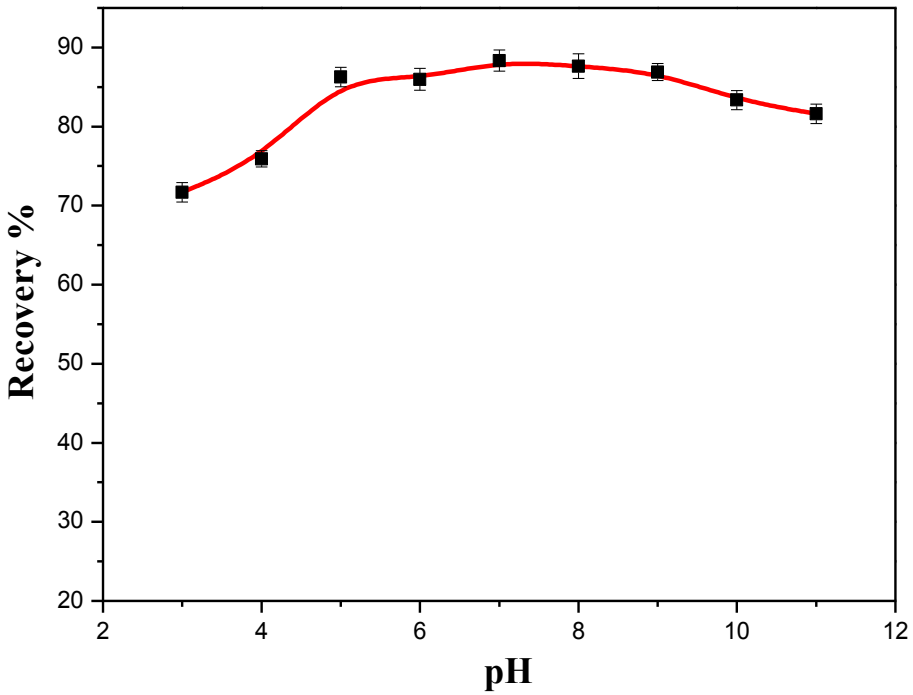

3.5. The Reusability of the Absorbent

The recycling of the nanoparticle adsorbents was studied to verify the chemical stability of the magnetic graphene composites. The Fe_3O_4@PDDA/GO*x*@DNA was prepared by a self-assembly technique, and the Fe_3O_4@PDDA/GO*x* was prepared by *in situ* synthesis. The adsorbents used in the adsorption procedure were treated with 2 mL of dichloromethane by ultrasonication for 10 min and then washed by 2 mL of *n*-hexane before being applied to the next adsorption procedure. The Fe_3O_4@PDDA/GO*x*@DNA adsorbents could be reused 20 times without losing much of the removal percentages of analytes (>80%, Figure 12). However, we found that if the absorbent used Fe_3O_4@SiO_2 as the carrier, it can be reused for at least 50 times, because it has good dispersibility.

Figure 12. The recycling efficiency *vs.* cycle number after removing BDE28 by Fe_3O_4@PDDA/GO*x*@DNA.

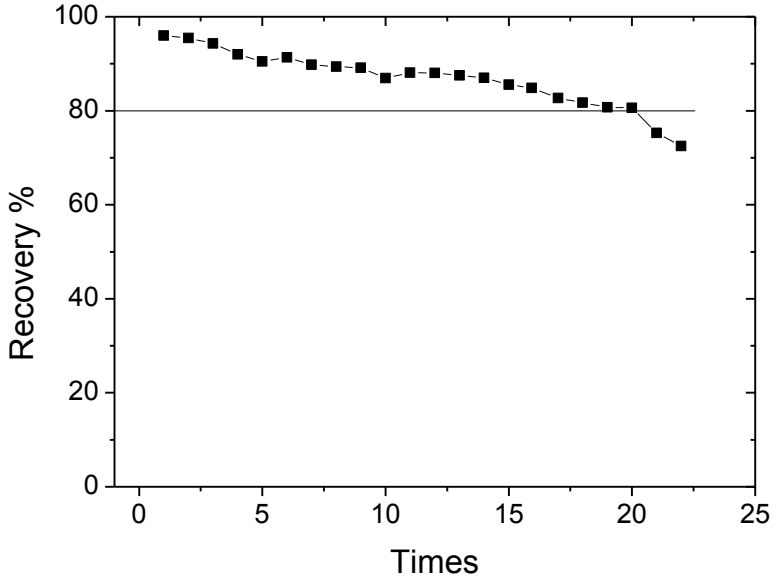

3.6. The Application of Adsorbent in Environmental Water Samples

To test the removal efficiency of Fe_3O_4@PDDA/GO*x*@DNA, tap water, Zhenhai River 1 and its spiked water samples (spiked with 5 ng/mL of BDEs), as well as Yongjiang River water were used as the analysis object by this paper. As shown in Table 2 and Figure 13, the results indicated that Zhenhai River water was contaminated by BDE 17, BDE28 and BDE 71 (Figure 13). The data of spiked water samples showed that Fe_3O_4@PDDA/GO*x*@DNA was a suitable material to remove BDEs in environmental water samples. The conventional method of C18 SPE (solid phase extraction with a C18 membrane) was used in our experiment, and the result implied that the adsorbents have excellent removal efficiency (Table 3).

Figure 13. Chromatographs of (**a**) Zhenhai River 1 sample and (**b**) the river sample spiked with 5 ng/mL of BDEs.

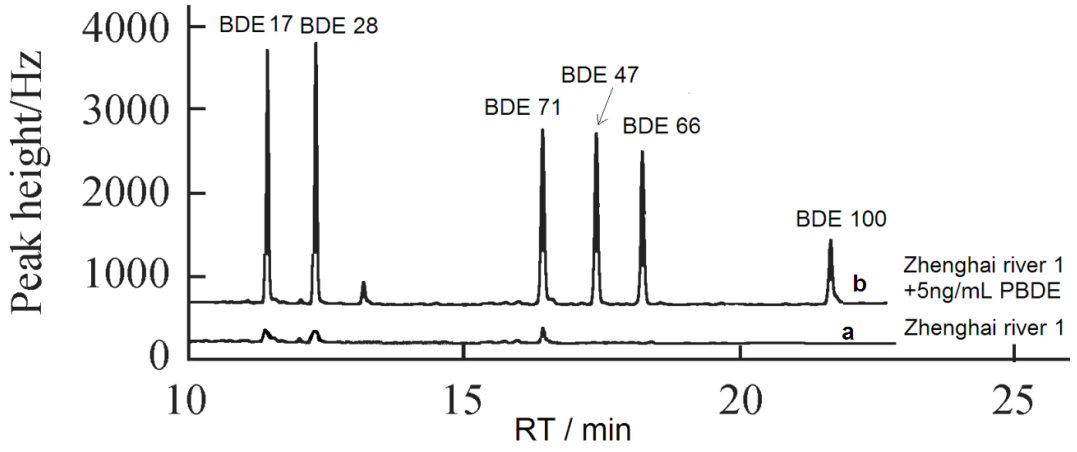

Table 3. The detection results of BDEs in Zhenhai River 2 water by the conventional method of C18 SPE and the proposed adsorbent in our manuscript.

Analytes in Zhenhai River 2		BDE17	BDE28	BDE71	BDE47	BDE66	BDE100
C18-SPE	Found (ng/mL)	0.50	0.58	0.69	ND	ND	ND
This work adsorbent	Found (ng/mL)	0.55	0.54	0.78	ND	ND	ND

4. Conclusions

In the present work, novel magnetic nanocomposites (Fe_3O_4@PDDA@DNA/GO*x*), using the facile layer-by-layer self-assembly method, were used as the adsorbents for removing six kinds of BDEs at the ng/mL order of magnitude in water samples. The method offered high specific removing efficiency to trace levels of BDEs and ease of operation by magnetic separation. More importantly, the magnetic nanocomposites have stable chemical properties and good reusability, which can be reused at least 20 times.

Acknowledgments

This work was supported by the National Natural Science Foundation of China (No. 31070866), the Natural Science Foundation of Zhejiang (LY13C200017, 2013A610163, 2012C37012), the Natural Science Foundation of Ningbo (2013A610241, 2013A610163), the Science and Technology Project of Zhejiang (2014A610184, 2013A610241, XYL10001, 2013C37033, 2012A610144, and 2011C50038) and the K.C. Wong Magna Fund in Ningbo University.

Author Contributions

Ning Gan design the main experimental scheme, idea and wrote most part of the paper, Jiabing Zhang and Shaichai Lin did all the chromatagraphia experiment and wrote part of the paper, Nengbing Long and Tianhua Li did all the characterization experiment. Yuting Cao design the part of the experimental scheme.

Conflicts of Interest

The authors declare no conflict of interest.

References

1. Hu, J.-W.; Zhuang, Y.; Luo, J.; Wei, X.-H.; Huang, X.-F. A theoretical study on reductive debromination of polybrominated diphenyl ethers. *Int*. *J*. *Mol*. *Sci*. **2012**, *13*, 9332–9342.
2. Hites, R.A. Polybrominated diphenyl ethers in the environment and in people: A meta-analysis of concentrations. *Environ*. *Sci*. *Technol*. **2004**, *38*, 945–956.
3. Moon, H.B.; Kannan, K.; Choi, M.; Yu, J.; Choi, H.G.; An, Y.R.; Choi, S.G.; Park, J.Y.; Kim, Z.G. Chlorinated and brominated contaminants including PCBs and BDEs in minke whales and common dolphins from Korean coastal waters. *J*. *Hazard*. *Mater*. **2010**, *179*, 35–41.

4. Meerts, I.A.T.M.; Letcher, R.J.; Hoving, S.; Marsh, G.; Bergman, Å.; Lemmen, J.G.; Burg, B.V.; Brouwer, A. *In vitro* estrogenicity of polybrominated diphenyl ethers, hydroxylated BDEs, and polybrominated bisphenol A compounds. *Environ*. *Health Perspect*. **2001**, *109*, 399–407.
5. Sears, K.; Dumée, L.; Schütz, J.; She, M.; Huynh, C.; Hawkins, S.; Duke, M.; Gray, S. Recent developments in carbon nanotube membranes for water purification and gas separation. *Materials* **2010**, *3*, 127–149.
6. Hu, Y.-C.; Hsu, W.-L.; Wang, Y.-T.; Ho, C.-T.; Chang, P.-Z. Enhance the pyroelectricity of polyvinylidene fluoride by graphene-oxide doping. *Sensors* **2014**, *14*, 6877–6890.
7. Chandra, V.; Park, J.; Chun, Y.; Lee, J.W.; Hwang, I.C.; Kim, K.S. Water-dispersible magnetite-reduced graphene oxide composites for arsenic removal. *ACS Nano* **2010**, *4*, 3979–3986.
8. Ai, L.-H.; Zhang, C.Y.; Chen, Z.-L. Removal of methylene blue from aqueous solution by a solvothermal-synthesized graphene/magnetite composite. *J*. *Hazard*. *Mater*. **2011**, *192*, 1515–1524.
9. Shao, L.-Y.; Yin, M.-J.; Tam, H.-Y.; Albert, J. Fiber optic pH sensor with self-assembled polymer multilayer nanocoatings. *Sensors* **2013**, *13*, 1425–1434.
10. Ling, X.Y.; Phang, I.Y.; Reinhoudt, D.N.; Vancso, G.J.; Huskens, J. Supramolecular layer-by-layer assembly of 3D multicomponent nanostructures via multivalent molecular recognition. *Int*. *J*. *Mol*. *Sci*. **2008**, *9*, 486–497.
11. Zeng, S.; Cao, Y.; Sang, W.; Li, T.; Gan, N.; Zheng, L. Enrichment of polychlorinated biphenyls from aqueous solutions using Fe_3O_4 grafted multiwalled carbon nanotubes with poly dimethyl diallyl ammonium chloride. *Int*. *J*. *Mol*. *Sci*. **2012**, *13*, 6382–6398.
12. Zhou, Y.L.; Li, Y.Z. Studies of the interaction between poly(diallyldimethyl ammonium chloride) and DNA by spectroscopic methods. *Colloids Surf*. *A* **2004**, *233*, 129–135.
13. Ma, Z.Y.; Guan, Y.P.; Liu, H.Z. Synthesis and characterization of micron-sized monodisperse superparamagnetic polymer particles with amino groups. *J*. *Polym*. *Sci*. *Part A Polym*. *Chem*. **2005**, *43*, 3433–3439.
14. Ke, F.; Qiu, L.G.; Yuan, Y.P.; Jiang, X.; Zhu, J.F. Fe_3O_4@MOF core-shell magnetic microspheres with a designable metal-organic framework shell. *J*. *Mater*. *Chem*. **2012**, *22*, 9497–9500.
15. Meng, L.; Gan, N.; Li, T.; Cao, Y.; Hu, F.; Zheng, L. A three-dimensional, magnetic and electroactive nanoprobe for amperometric determination of tumor biomarkers. *Int*. *J*. *Mol*. *Sci*. **2011**, *12*, 362–375.
16. Park, J.H.; Dao, T.D.; Lee, H.-I.; Jeong, H.M.; Kim, B.K. Properties of graphene/shape memory thermoplastic polyurethane composites actuating by various methods. *Materials* **2014**, *7*, 1520–1538.
17. Zhu, M.; Diao, G. Review on the progress in synthesis and application of magnetic carbon nanocomposites. *Nanoscale* **2011**, *3*, 2748–2767.
18. Zhou, J.; Romero, G.; Rojas, E.; Ma, L.; Moya, S.; Gao, C. Layer by layer chitosan/alginate coatings on poly(lactide-co-glycolide) nanoparticles for antifouling protection and Folic acid binding to achieve selective cell targeting. *J*. *Colloid Interface Sci*. **2010**, *345*, 241–247.
19. Sukhorukov, G.B.; Donath, E.; Lichtenfeld, H.; Knippel, E.; Knippel, M.; Budde, A.; Mohwald, H. Layer-by-layer self assembly of polyelectrolytes on colloidal particles. *Colloids*. *Surf*. *A Physicochem*. *Eng*. *Aspects* **1998**, *137*, 253–266.

20. Hammond, P.T. Engineering materials layer-by-layer: Challenges and opportunities in multilayer assembly. *AIChE J*. **2011**, *57*, 2928–2940.
21. Zhu, J.H.; Chen, J.-L.; He, L.; Zhao, L.; Li, S.-Y.; Guo, Z.H. An overview of the engineered graphene nanostructures and nanocomposites. *RSC Adv*. **2013**, *3*, 22790–22824.
22. Zhu, J.; Luo, Z.; Wu, S.; Haldolaarachchige, N.; Young, D.P.; Wei, S.; Guo, Z. Magnetic graphene nanocomposites: Electron conduction, giant magnetoresistance and tunable negative permittivity. *J. Mater. Chem*. **2012**, *22*, 835–844.